Original article

Folia Neuropathologica

Size frequency distributions of β-amyloid (Aβ) deposits: a comparative study of four neurodegenerative disorders

Richard A. Armstrong

Vision Sciences, Aston University, Birmingham, UK

Folia Neuropathol 2012; 50 (3): 240-249 DOI: 10.5114/fn.2012.30524

Abstract

Deposition of β-amyloid (Aβ), a 'signature' pathological lesion of Alzheimer's disease (AD), is also characteristic of Down's syndrome (DS), and has been observed in dementia with Lewy bodies (DLB) and corticobasal degeneration (CBD). To determine whether the growth of Aβ deposits was similar in these disorders, the size frequency distributions of the diffuse ('pre-amyloid'), primitive ('neuritic'), and classic ('dense-cored') Aβ deposits were compared in AD, DS, DLB, and CBD. All size distributions had essentially the same shape, i.e., they were unimodal and positively skewed. Mean size of Aβ deposits, however, varied between disorders. Mean diameters of the diffuse, primitive, and classic deposits were greatest in DS, DS and CBD, and DS, respectively, while the smallest deposits, on average, were recorded in DLB. Although the shape of the frequency distributions was approximately log-normal, the model underestimated the frequency of smaller deposits and overestimated the frequency of larger deposits in all disorders. A 'power-law' model fitted the size distributions of the primitive deposits in AD, DS, and DLB, and the diffuse deposits in AD. The data suggest: (1) similarities in size distributions of Aβ deposits among disorders, (2) growth of deposits varies with subtype and disorder, (3) different factors are involved in the growth of the diffuse/primitive and classic deposits, and (4) log-normal and power-law models do not completely account for the size frequency distributions.

Key words: *β-amyloid (Aβ), size frequency distribution, log-normal distribution, surface diffusion.*

Introduction

β-amyloid (Aβ) deposition in the form of diffuse ('pre-amyloid'), primitive ('neuritic'), and classic ('dense-cored') deposits is a 'signature' pathological feature of Alzheimer's disease (AD) [4,6,9,24,28]. Aβ deposition is also an important aspect of the pathology of Down's syndrome (DS) due to the triplication of the amyloid precursor protein (APP) gene on chromosome 21 [15,28]. In addition, Aβ has been reported as an additional pathology in dementia with Lewy bodies (DLB) [18], Parkinson's disease (PD) [50], Pick's disease (PiD) [50], corticobasal degeneration (CBD) [11,50], amyotrophic lateral sclerosis (ALS) (Hamilton and Bouser 2004), and progressive supranuclear palsy (PSP) [50].

Aβ is generated via β- and γ-secretase cleaving of APP resulting in the formation of an aggregated protein deposit. Three processes are involved in the formation of such deposits: (1) an initial nucleation event, (2) a nucleated polymerization reaction, and (3) the growth of newly formed nuclei into larger aggregates [22,31,36].

Communicating author:
Dr. R.A. Armstrong, Vision Sciences, Aston University, Birmingham B4 7ET, UK, phone 0121-359-3611, fax 0121-333-4220, e-mail: R.A.Armstrong@aston.ac.uk

Several studies suggest that once initiated, Aβ deposits in AD grow in size over time. First, pseudo colour image processing of Aβ deposits in AD reveal gradients of density consistent with growth from a central point [21]. Second, radioiodinated human Aβ can be deposited experimentally *in vitro* from a dilute solution onto primitive and diffuse Aβ deposits causing them to grow [38]. Third, in transgenic mice, Aβ deposits appear in clusters which grow in size from 14 μm at 8 months to 22 μm at 12 months [54,55]. Fourth, transgenic studies also suggest that increasing accumulation of Aβ is largely by growth of existing deposits rather than by further nucleation [47].

A statistical mechanics approach has been used to model the growth of Aβ deposits in AD [52,54,55]. Two factors have been identified that influence growth: (1) addition and removal of Aβ ('aggregation/disaggregation') and (2) 'surface diffusion' [52]. During aggregation, monomers of Aβ interact to form more complex oligomers resulting in deposit growth. During disaggregation, Aβ molecules are removed from a deposit by glial cells resulting in shrinkage of a deposit. The ultimate size of an Aβ deposit therefore depends on the balance between aggregation and disaggregation. Surface diffusion describes a process by which additional molecular constituents are acquired by an Aβ deposit by diffusion through the neuropil and molecular binding to Aβ [7,19,54,55]. Several proteins associated with Aβ deposits could have been acquired by this process including amyloid-P, α-antichymotrypsin, complement factors, and apolipoprotein E (Apo E) [9,49], and could influence deposit growth and morphology. The processes of aggregation/disaggregation and surface diffusion result in characteristic size frequency distributions of the resulting Aβ deposits [32,54,55]. Hence, the size frequency distribution of Aβ deposits can be described by a 'power-law' model if aggregation/disaggregation predominates over surface diffusion and a 'log-normal' model if surface diffusion is the predominant factor [54,55].

The present study compared the size frequency distributions of Aβ deposits in the temporal lobe of four disorders in which Aβ is deposited under different pathological conditions, viz., AD, DS, DLB, and CBD. AD and CBD are tauopathies and DLB is a synucleinopathy [29], while in DS, Aβ results from triplication of the *APP* gene. The specific objectives were to determine: (1) whether the size distributions were similar in different disorders, (2) whether the size frequency distributions could be described by log-normal or power-law models, and hence, (3) whether growth of Aβ deposits in the various disorders could be completely explained by aggregation/disaggregation and surface diffusion.

Material and methods

Cases

Cases (details in Table I) were obtained from the Brain Bank, Department of Neuropathology, Institute of Psychiatry, King's College, London, UK. Informed consent was given for the removal of all brain tissue according to the 1996 Declaration of Helsinki (as modified Edinburgh 2000). AD cases (*N* = 10) all fulfilled 'National Institute of Neurological and Communicative Disorders and Stroke and the Alzheimer Disease and Related Disorders Association' (NINCDS/ADRDA) criteria for probable AD [53] and neuropathologically verified using 'Consortium to Establish a Registry of Alzheimer Disease' (CERAD) criteria [41] and National Institute on Aging and Reagan Institute criteria [20,33]. Clinically assessed and karyotyped DS cases (*N* = 12) were referred from the Bethlem Royal and Maudsley Hospital and

Table I. Demographic details of the cases used in the study

Disorder	*N*	M : F	Mean age at death; years (range, SD)	Mean disease duration; years (range, SD)
Alzheimer's disease	10	2 : 8	80.2 (64-93, 8.5)	5.9 (2-16, 3.3)
Down's syndrome	12	5 : 1	40.7 (38-47, 4.03)	–
Dementia with Lewy bodies	8	8 : 0	73.5 (69-77, 3.70)	7.0 (3-18, 6.0)
Corticobasal degeneration	3	1 : 2	65.5 (54-81, 10.01)	–

N – number of cases studied, M – male, F – female, SD – standard deviation

St. Mary's Hospital, London, UK [15]. DLB cases (N = 8) were diagnosed according to the 'Consortium on Dementia with Lewy bodies' (CDLB) guidelines [40] and possessed significant numbers of Aβ deposits. There is no specific clinical phenotype characteristic of CBD as diverse presentations of the disease are present [25]. However, the pathology of the cases (N = 3) was consistent with the criteria recommended by the National Institute of Health (NIH) Office of Rare Diseases for the pathological diagnosis of CBD [25]. First, tau-immunoreactive neuronal cytoplasmic inclusions (NCI) were present, glial inclusions (GI) in oligodendrocytes, and extensive inclusions within the processes or 'threads' of astrocytes ('astrocytic plaques'). Second, NCI and GI were present in the white and grey matter of various cortical regions and in the striatum. Third, neuronal loss was present in focal cortical areas and in the substantia nigra.

Histological methods

A block of the temporal cortex was taken from each case at the level of the lateral geniculate nucleus to study the superior temporal gyrus (B22), inferior temporal gyrus (B20), and parahippocampal gyrus (B28), regions which have high densities of Aβ deposits in the disorders studied [10,11,15,18]. Tissue was fixed in 10% phosphate buffered formal-saline and embedded in paraffin wax. 7 μm coronal sections were stained with a rabbit polyclonal antibody (Gift of Prof. B.H. Anderton, Institute of Psychiatry, King's College London) raised to the 12-28 amino acid sequence of the Aβ protein [51]. The antibody was used at a dilution of 1 in 1200 and the sections incubated at 4°C overnight. Sections were pretreated with 98% formic acid for 6 minutes which enhances Aβ immunoreactivity. Aβ was visualised using the streptavidin-biotin horseradish peroxidase procedure with diaminobenzidine as the chromogen. Sections were also stained with haematoxylin.

Morphometric methods

In each gyrus studied, the greatest diameters of a sample of diffuse, primitive, and classic Aβ deposits were measured. Guidelines were marked on the slide parallel to the pia mater to sample laminae II/III and V/VI, which contain the most significant numbers of deposits [2]. The maximum diameter of each Aβ deposit touching a guideline was then measured at a magnification of ×400 using an eyepiece micrometer. The three most common morphological subtypes of Aβ deposit were identified using previously defined criteria [4,24]. Hence, diffuse Aβ deposits were 10-200 μm in diameter, irregular in shape, had diffuse boundaries, and were lightly immunolabelled. Large confluent patches of Aβ immunolabelling, which could be a variant of diffuse deposit, were not quantified. Primitive deposits were 20-60 μm, well demarcated, more symmetrical in shape than diffuse deposits, and strongly immunolabelled and may be analogous to the neuritic plaques (NP), the predominant type of plaque in AD [26,27]. Classic deposits were 20-100 μm, had a distinct central 'core' surrounded by a 'corona' of dystrophic neurites. Within a disorder, there were no significant differences in size distributions between cases and brain regions within a case. Hence, to obtain a sufficiently large sample of each Aβ deposit type of each disorder for analysis, measurements were pooled from all brain regions and cases.

Data analysis

Two statistical models were fitted to the data using STATISTICA software (Statsoft Inc., 2300 East 14th St, Tulsa, OK74104, USA). First, a 'power-law' model was fitted to each size distribution. A variable (Y) is distributed as a power-law function of X if the dependent variable has an exponent 'a', i.e., a function of the form $Y = CX^{-a}$. If the data are fitted by such a function, a plot of log (Y) against log (X) should yield a linear relationship. Hence, for each region, deposit sizes were grouped into classes and the logarithm of the frequency of the deposits in each class was plotted against the logarithm of the upper size limit of the class. A linear function was then fitted to the data and the goodness of fit to a linear model tested using Pearson's correlation coefficient ('r'). Second, a log-normal model was fitted to the size distribution of each type of deposit from each disorder. This distribution is defined as that of a variable X such that the natural logarithm (ln) of $(X - \varnothing)$ is normally distributed [45]. The distribution has three parameters: $\varnothing$ (where $X > \varnothing$), the mean (μ), and the variance (σ^2). In many applications, the value of $\varnothing$ can be assumed to be zero and a two-parameter model fitted to the data. Deviations from a log-normal model were tested using the Kolmogorov-Smirnov (KS) goodness of fit test. Size frequency distributions were compared between disorders using chi-square (χ^2) contingency table tests. In addition, mean diameters of each type of deposit were compared among disorders using one-way analysis of variance (ANOVA) and

Fisher's protected least significant difference (PLSD) as a *post-hoc* procedure [13].

Results

The size distributions of the diffuse, primitive, and classic Aβ deposits in each disorder are shown in Figs. 1-3. The distributions, regardless of subtype or disorder, had similar shapes, i.e., they were unimodal and exhibited a significant degree of positive skew. There were few Aβ deposits in the smallest size classes, maximum frequency occurred within a single size class (the modal class), and the frequency of the larger deposits declined with increasing size. The mean size, modal class, standard deviation (SD), and degree of skew of the size distributions of Aβ deposits in AD, DS, DLB, and CBD are shown in Table II. Diffuse Aβ deposits were on average larger than the primitive and classic deposits and exhibited the greatest degree of skew. The primitive A deposits were often the smallest deposits present. The mean diameters of the diffuse (F = 282.83, P < 0.001), primitive (F = 97.20, P < 0.001), and classic (F = 15.47, P < 0.001) varied among disorders. The mean diameter of the diffuse Aβ deposits was greatest in DS and least in DLB while the mean diameter of the primitive deposits was greatest in DS and CBD and least in DLB. The mean diameter of the classic Aβ deposits was greatest in DS and least in CBD.

The size frequency distributions of the diffuse, primitive, and classic Aβ deposits in the four disorders are shown in Figs. 1-3. There were significant differences in size frequency distribution among disorders for all deposit types: (1) DS had a significantly higher proportion of larger diffuse deposits and DLB a higher proportion of smaller diffuse deposits than either AD or CBD, which had similar size distributions of diffuse deposits (Fig. 1), (2) DS had the highest proportion of larger primitive deposits, followed by CBD, AD, and DLB (Fig. 2), the primitive deposits in AD having a particularly restricted size range, and (3) classic deposits reached their greatest size in DS, followed by AD, with DLB and CBD having a higher proportion of smaller classic deposits.

The result of fitting a log-normal distribution to the diffuse Aβ deposits in AD is shown in Figure 4. The distribution is approximately log-normal in shape but also deviates significantly from the model in some size classes (KS = 0.16, P < 0.01). Hence, the frequency of the

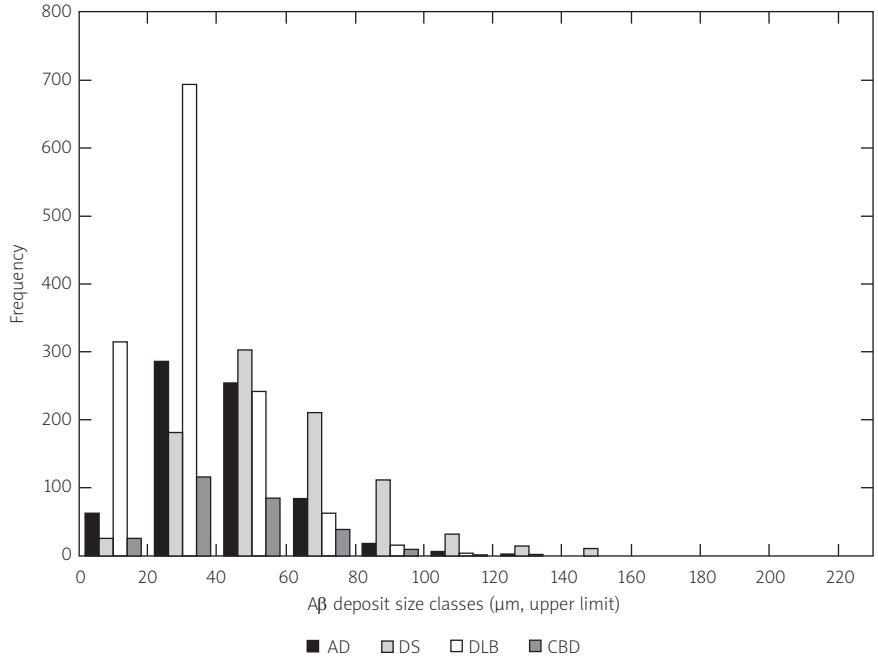

AD – Alzheimer's disease, DS – Down's syndrome, DLB – dementia with Lewy bodies, CBD – corticobasal degeneration

Fig. 1. Size frequency distributions of the diffuse β-amyloid (Aβ in four neurodegenerative disorders. Chi-square (χ^2) contingency table analysis comparing disorders: AD/DS χ^2 = 194.23 (13 DF, P < 0.001), DS/DLB χ^2 = 695.12 (13 DF, P < 0.001), DLB/CBD χ^2 = 112.58 (13 DF, P < 0.001), AD/DLB χ^2 = 193.46 (13 DF, P < 0.001), DS/CBD χ^2 = 93.66 (13 DF, P < 0.001, AD/CBD χ^2 = 11.81 (13 DF, P > 0.05).

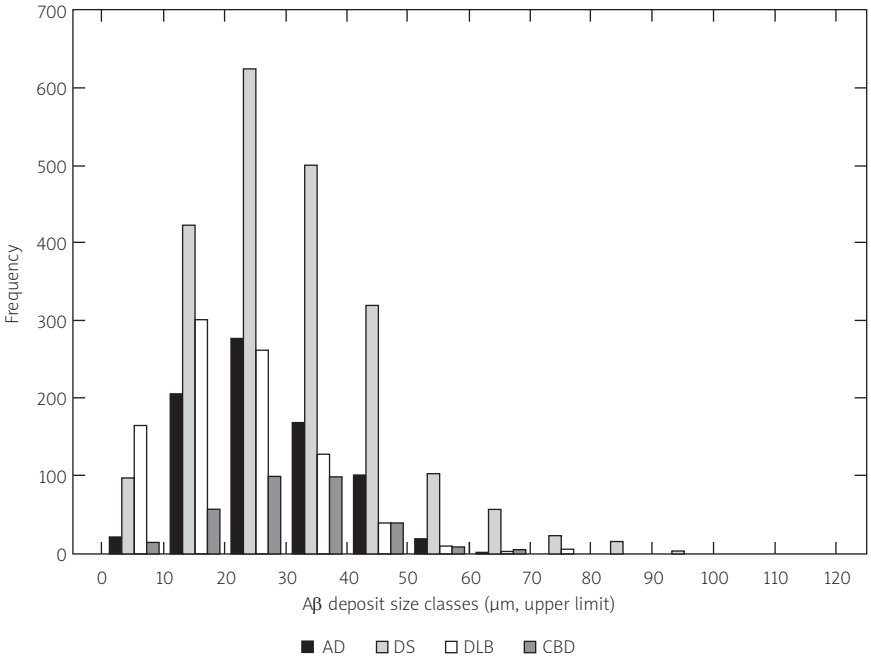

AD – Alzheimer's disease, DS – Down's syndrome, DLB – dementia with Lewy bodies, CBD – corticobasal degeneration

Fig. 2. Size frequency distributions of the primitive β-amyloid (Aβ in four neurodegenerative disorders. Chi-square (χ^2) contingency table analysis comparing disorders: AD/DS χ^2 = 62.10 (10 DF, $P < 0.001$), DS/DLB χ^2= 8.9 (10 DF, $P < 0.001$), DLB/CBD χ^2 = 122.74 (7 DF, $P < 0.001$), AD/DLB χ^2 = 163.26 (9 DF, $P < 0.001$), DS/CBD χ^2 = 14.61 (7 DF, $P < 0.05$), AD/CBD χ^2 = 25.25 (7 DF, $P < 0.001$).

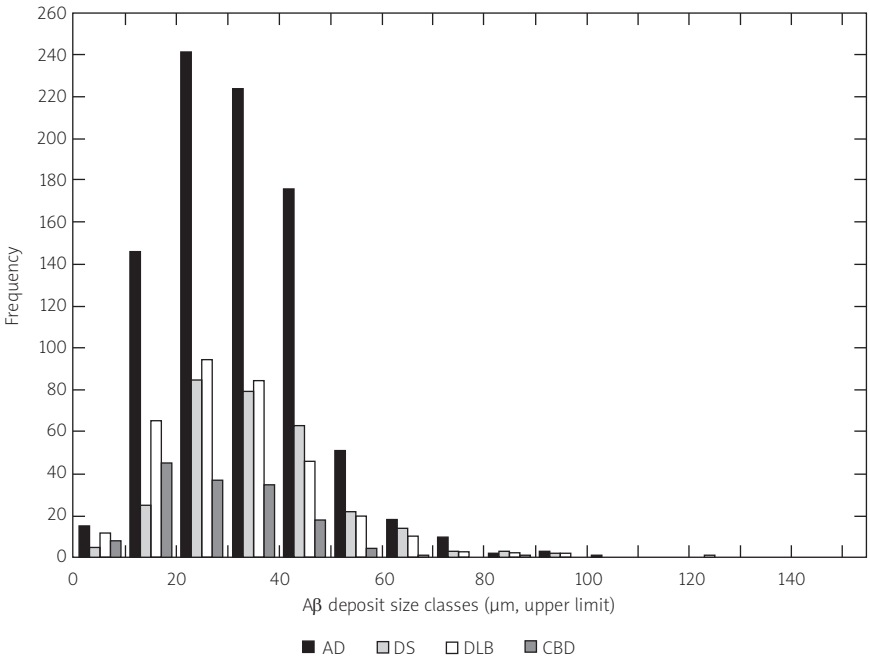

AD – Alzheimer's disease, DS – Down's syndrome, DLB – dementia with Lewy bodies, CBD – corticobasal degeneration

Fig. 3. Size frequency distributions of the classic β-amyloid (Aβ in four neurodegenerative disorders. Chi-square (χ^2) contingency table analysis comparing disorders: AD/DS χ^2= 4.20 (11 DF, $P < 0.05$), DS/DLB χ^2 = 22.80 (9 DF, $P < 0.01$), DLB/CBD χ^2 = 3.74 (9 DF, $P > 0.05$), AD/DLB χ^2 = 13.06 (10 DF, $P > 0.05$), DS/CBD χ^2= 51.54 (9 DF, $P < 0.001$), AD/CBD χ^2 = 32.08 (9 DF, $P < 0.001$).

Table II. Summary statistics for the size frequency distributions of the diffuse, primitive, and classic β-amyloid (Aβ) deposits in four neurodegenerative disorders

Group	Deposit type	*N*	Mean (μm)	Mode (μm)	Median (mm)	SD (μm)	Skew
AD	Diffuse	715	47.22	50	45	20.01	1.20**
	Primitive	796	31.58	30	30	11.76	0.65*
	Classic	888	37.02	30	35	14.52	0.88**
DS	Diffuse	898	64.34	50	60	27.89	1.03**
	Primitive	2177	35.29	30	30	15.80	0.97*
	Classic	302	40.52	30	40	16.36	1.26**
DLB	Diffuse	1340	36.56	30	30	18.35	1.62**
	Primitive	921	25.74	20	20	13.18	1.38*
	Classic	338	35.65	30	30	15.83	0.98**
CBD	Diffuse	285	49.28	40	45	23.07	1.41**
	Primitive	326	32.60	30	30	12.44	0.41**
	Classic	149	14.90	20	25	13.59	0.86**

AD – Alzheimer's disease, DS – Down's syndrome, DLB – dementia with Lewy bodies, CBD – corticobasal degeneration
N – number of deposits sampled, SD – standard deviation
**P < 0.05, **P < 0.01*
Analysis of variance (ANOVA): One-way with 'Fisher's protected least significant difference' (PLSD) post-hoc procedure: Diffuse Aβ deposits F = 282.83 (P < 0.001), DS > CBD = AD > DLB; Primitive Aβ deposits F = 97.20 (P < 0.001), DS = CBD > AD > DLB; Classic Aβ deposits F = 15.47 (P < 0.001), DS > AD = DLB > CBD

smaller Aβ deposits was greater than predicted by the model, there were more deposits than expected in the modal class, and there were fewer deposits than expected in the larger size classes. Goodness-of-fit of the log-normal distribution to all disorders and Aβ subtypes is shown in Table III. Size distributions, regardless of subtype or disorder, exhibited a similar pattern of deviation from a log-normal distribution, the model underestimating the frequency of smaller deposits and overestimating the frequency of larger deposits.

An example of fitting a power-law model to the size distributions of the primitive Aβ deposits in DLB is shown in Figure 5. There is a statistically significant fit to this model ($r = -0.86$, $P < 0.01$). Nevertheless, the data also depart from a power-law model, viz., there were fewer Aβ deposits than predicted in the smallest size classes, more than expected in the intermediate size classes, and fewer in the largest size classes. A significant fit to a power-law model was obtained for 5/12 (42%) of the size distribution studied, viz., the primitive deposits in AD, DS, and DLB and the diffuse deposits in AD. All size distributions, however, exhibited similar departures from a power-law model, the model overestimating the frequency of the smallest and largest deposits.

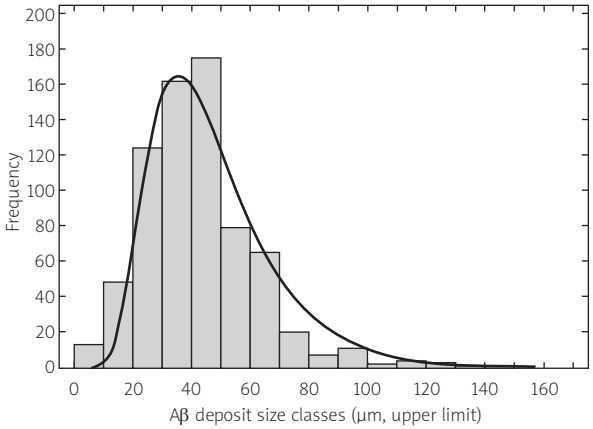

Fig. 4. Goodness of fit of the size frequency distribution of the diffuse β-amyloid (Aβ) deposits in Alzheimer's disease (AD) to a 'log-normal' model. Deviation from model: KS = 0.16, $P < 0.01$.

Table III. Size class frequency distributions of diffuse, primitive, and classic β-amyloid (Aβ) deposits in various neurodegenerative disorders

Disorder	Subtype	Deviation from log-normal model (KS)	Fit to power-law model ('r')
AD	Diffuse	0.16**	–0.61*
	Primitive	0.17**	–0.77**
	Classic	0.14 **	–0.56 ns
DS	Diffuse	0.13**	–0.59 ns
	Primitive	0.17**	–0.68**
	Classic	0.14**	–0.57 ns
DLB	Diffuse	0.11**	–0.41 ns
	Primitive	0.15**	–0.86**
	Classic	0.15 **	–0.57 ns
CBD	Diffuse	0.14 **	–0.42 ns
	Primitive	0.18**	–0.49 ns
	Classic	0.12*	–0.57 ns

AD – Alzheimer's disease, DS – Down's syndrome, DLB – dementia with Lewy bodies, CBD – corticobasal degeneration
Goodness of fit to log-normal and power-law models: KS – Kolmogorov-Smirnov statistic, 'r' – Pearson's correlation coefficient
**P < 0.05, **P < 0.01, ns – not significant*

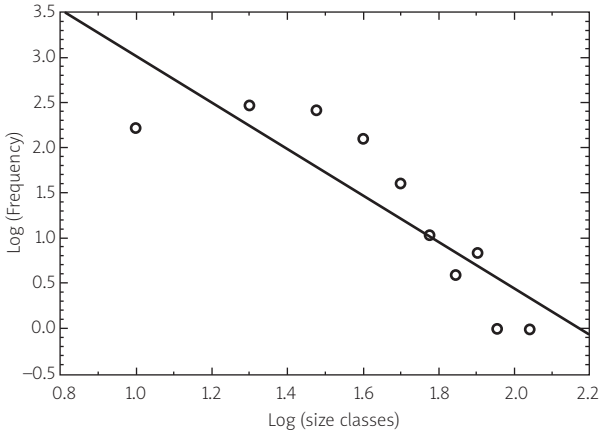

Fig. 5. Goodness of fit of the size frequency distribution of the primitive β-amyloid (Aβ) deposits in Down's syndrome (DS) to a 'power-law' model. Fit to model: $r = –0.86$, $P < 0.01$.

Discussion

There are two problems in estimating the size distributions of Aβ deposits which exist in three dimensions (3D) measured in a single plane. First, sampling in two dimensions (2D) underestimates the frequency of the smaller deposits and overestimates the frequency of the larger deposits [16,34]. Second, the section cuts through different portions of the deposit, i.e., some small diameter measurements represent sections taken through the peripheral portions of larger-sized deposits [14]. The absolute density of deposits in each size class in 3D can be calculated from their size distribution in 2D using matrix algebra if it is assumed that the deposits are spherical and randomly distributed [23,48,56]. However, this method is not appropriate for Aβ deposits, because although many deposits may be approximately spherical, they are not randomly distributed but occur in distinct clusters [10,12]. The effect of sampling in 2D on the size frequency distributions of Aβ deposits has been studied in AD [16]. Using data from a sample of brain regions, the size distributions of Aβ deposits in single sections were compared with their distribution in a volume of tissue by serial reconstruction through the tissue. The data suggested that the two sources of bias cancel out and that therefore, the errors involved in estimating the size distribution of protein aggregates in 3D by 2D sampling are relatively small [16].

All size frequency distributions, regardless of morphological subtype or disorder, were asymmetric and positively skewed similar to previous reports of Aβ de-

posits in AD [8,32]. These results suggest similarities in the growth of Aβ deposits in the different disorders. Nevertheless, there were differences among disorders including in mean diameter, degree of skew, and in length of the tail of the distribution. The largest diffuse and classic deposits occurred in DS, while the diffuse and primitive deposits in DLB and classic deposits in CBD exhibited the least growth potential. In DS, deposits may grow more rapidly or develop over a much longer time period compared with the other disorders. First, Aβ deposition in DS is associated with triplication of the *APP* gene, which may result in overproduction of Aβ and therefore, faster-growing and larger deposits. Second, virtually all patients with DS develop Aβ deposits if they survive into their thirties [15,39,43,57], with particular accumulations of deposits observed between the ages of 30 and 50 years [32]. Hence, Aβ deposits in DS may develop over longer periods than in AD, DLB, and CBD. The smallest deposits were observed in DLB and CBD. The rate of progression of disease may be faster in these disorders than in AD or DS resulting in less time for deposit growth [44]. Alternatively, Aβ deposition in DLB and CBD could be related to the onset of dementia which may occur later in parkinsonian syndromes than in AD or DS [46].

Development of Aβ deposits is influenced by at least two processes, viz., aggregation/disaggregation of Aβ and surface diffusion followed by molecular binding to Aβ [52,54,55]. In all four disorders, although size distributions approximated to a log-normal distribution, they also deviated from the model, Aβ deposits appearing to grow less in all disorders than predicted. Various factors could restrict growth of an Aβ deposit. For example, growth could be limited by the lack or insufficient quantity of a suitable 'chaperone' molecule [35,37], inhibited diffusion of the molecule through the neuropil, failure of the molecule to penetrate sufficiently into an Aβ deposit, or failure to bind to Aβ [17].

A power-law model fitted the size distributions of the diffuse and primitive Aβ deposits in AD and the primitive deposits in DS and DLB. In AD and DS, diffuse deposits are spatially correlated with neuronal cell bodies [1,5,42]. Development of diffuse deposits may therefore involve: (1) secretion of Aβ monomers from clusters of adjacent neuronal perikarya, (2) association of Aβ monomers to form more complex oligomers, and (3) formation of an aggregated deposit [5,21]. Further condensation of the deposit and its association with neuritic pathology, in the form of dystrophic neuritis (DN), may then result in the formation of a primitive-type Aβ deposit [4]. Disaggregation within a deposit may also occur as a result of the removal of Aβ monomers by glial cells which are frequently embedded within and present at the periphery of many diffuse and primitive deposits [17]. Nevertheless, some size distributions, most notably those of the classic Aβ deposits in all disorders and all deposit subtypes in CBD, were not fitted successfully by a power-law model suggesting additional factors were involved in growth. Classic deposits are frequently spatially associated with blood vessels, and substances diffusing from blood vessels may influence growth [3,7]. In addition, CBD is a four-repeat (4R) tauopathy with extensive neuritic degeneration in the form of NCI, GI, and astrocytic plaques [25]. Hence, in CBD, there may be a greater chance that a diffuse Aβ deposit will combine with neuritic elements to form a primitive deposit.

In conclusion, the shape of the size frequency distributions of diffuse, primitive, and classic Aβ deposits show considerable similarities in AD, DS, DLB, and CBD. Nevertheless, Aβ deposits exhibit differences in growth potential between disorders, diffuse and classic deposits in DS exhibiting the greatest growth and diffuse deposits in DLB and classic deposits in CBD the least growth. Although both aggregation/disaggregation and surface diffusion may play a role in deposit growth, all size distributions deviated to some extent from previously described models suggesting additional factors must be involved.

Acknowledgements

The assistance of the Brain Bank, Institute of Psychiatry, King's College London in preparation of tissue sections for this study are gratefully acknowledged.

References

1. Allsop D, Haga S, Ikeda SI, Mann DMA, Ishii T. Early senile deposits in Down's syndrome brains show a close relationship with cell bodies of neurons. Neuropathol Appl Neurobiol 1989; 15: 531-542.
2. Armstrong RA. Correlations between the morphology of diffuse and primitive β-amyloid (Aβ) deposits and the frequency of associated cells in Down's syndrome. Neuropath Appl Neurobiol 1996a; 22: 527-530
3. Armstrong RA. β-amyloid (Aβ) deposits and blood vessels: laminar distribution in the frontal cortex of patients with Alzheimer's disease. Neurosci Res Communs 1996b; 18: 19-28.
4. Armstrong RA. β-amyloid plaques: stages in life history or independent origin? Dement Geriatr Cogn Disord 1998; 9: 227-238.
5. Armstrong RA. Diffuse β-amyloid (Aβ) deposits and neurons: *in situ* secretion or diffusion of Aβ. Alz Rep 2001; 3: 289-294.

6. Armstrong RA. Plaques and tangles and the pathogenesis of Alzheimer's disease. Folia Neuropathol 2006a; 44: 1-11.
7. Armstrong RA. Classic β-amyloid deposits cluster around large diameter bloodvessels rather than capillaries in sporadic Alzheimer's disease. Curr Neurovasc Res 2006b; 3: 289-294.
8. Armstrong RA. Size frequency distributions of abnormal protein deposits in Alzheimer's disease and variant Creutzfeldt-Jakob disease. Folia Neuropathol 2007; 45: 108-114.
9. Armstrong RA. The molecular biology of senile plaques and neurofibrillary tangles in Alzheimer's disease. Folia Neuropathol 2009; 7: 289-299.
10. Armstrong RA. A spatial pattern analysis of β-amyloid (Aβ) deposition in the temporal lobe in Alzheimer's disease. Folia Neuropathol 2010; 48: 67-74.
11. Armstrong RA. Density and spatial pattern of β-amyloid (Aβ) deposits in corticobasal degeneration. Folia Neuropathol 2011a; 49: 14-20.
12. Armstrong RA. Spatial patterns of β-amyloid (Aβ) deposits in familial and sporadic Alzheimer's disease. Folia Neuropathol 2011b; 49: 153-161.
13. Armstrong RA, Hilton A. Statistical Analysis in Microbiology: Statnotes. Wiley-Blackwell, Hoboken 2011.
14. Armstrong RA, Myers D, Smith CUM. Alzheimer's disease: size class frequency distribution of senile plaques: do they indicate when a brain region was affected? Neurosci Lett 1991; 127: 223-226.
15. Armstrong RA, Smith CUM. β-amyloid (Aβ) deposition in the medial temporal lobe in Down's syndrome: effects of brain region and patient age. Neurobiol Dis 1995; 1: 139-144.
16. Armstrong RA, Myers D, Smith CUM. Factors determining the size frequency distribution of β-amyloid (Aβ) deposits in Alzheimer's disease. Exp Neurol 1997; 145: 574-579.
17. Armstrong RA, Cairns NJ, Lantos PL. Degeneration of cortical neurons associated with diffuse β-amyloid (Aβ) deposits in Alzheimer's disease. Neurosci Res Communs 1999; 24: 89-97.
18. Armstrong RA, Cairns NJ, Lantos PL. Beta-amyloid deposition in the temporal lobe of patients with dementia with Lewy bodies: Comaprison with non-demented cases and Alzheimer's disease. Dement Geriatr Cogn Disord 2000; 11: 187-192.
19. Armstrong RA, Lantos PL, Cairns NJ. What determines the molecular composition of abnormal protein aggregates in neurodegenerative disease? Neuropathology 2008; 28: 351-365.
20. Ball M, Braak H, Coleman P, Dickson D, Duyckaerts C, Gambetti P, Hansen L, Hyman B, Jellinger K, Markesbery W, perl D, Powers J, Price J, Trojanowski JQ, Wisniewski H, Phelps C, Khachaturian Z. Consensus recommendations for the postmortem diagnosis of Alzheimer's disease. Neurobiol Aging 1997; 18: S1-S2.
21. Benes FM, Reifel JL, Majocha RE, Marotta CA. Evidence for a diffusional model of Alzheimer amyloid A4 (β amyloid) during neuritic plaque formation. Neuroscience 1989; 33: 483-488.
22. Christopeit T, Hortschansky P, Schroeckh V, Guhrs K, Zandomeneghi G, Fandrich M. Mutagenic analysis of the nucleation propensity of oxidized Alzheimer's beta-amyloid peptide. Protein Sci 2005; 14: 2125-2131.
23. Cruz-Orive J. Distribution-free estimation of sphere size distribution from slabs showing overprojections and truncation, with a review of previous methods. J Microsc 1983; 131: 265-290.
24. Delaere P, Duyckaerts C, He Y, Piette F, Hauw JJ. Subtypes and differential laminar distribution of β/A4 deposits in Alzheimer's disease: Relationship with the intellectual status of 26 cases. Acta Neuropathol 1991; 81: 328-335.
25. Dickson DW, Bergeron C, Chin SS, Duyckaerts C, Horoupian D, Ikeda K, Jellinger K, Lantos PL, Lippa CF, Mirra SS, Tabaton M, Vonsattel JP, Wakabayashi K, Litvan I. Office of rare diseases neuropathologic criteria for corticobasal degeneration. J Neuropath Exp Neurol 2002; 61: 935-946.
26. Gibson PH. Relationship between numbers of cortical argentophilic and congophilic senile plaques in the brains of elderly people with and without senile dementia of the Alzheimer type. Gerontology 1985; 31: 321-324.
27. Gibson PH. Ultrastructural abnormalities in the cerebral neocortex and hippocampus associated with Alzheimer's disease and aging. Acta Neuropathol 1987; 73: 86-91.
28. Glenner GG, Wong CW. Alzheimer's disease and Down's syndrome: sharing of a unique cerebrovascular amyloid fibril protein. Biochem Biophys Res Commun 1984; 122: 1131-1135.
29. Goedert M. The significance of tau and α-synuclein inclusions in neurodegenerative disease. Curr Opin in Genetics and Dev 2001; 11: 343-351.
30. Hamilton RL, Bouser R. Alzheimer's disease pathology in amylotrophic lateral sclerosis. Acta Neuropathol 2004; 107: 515-522.
31. Harper JD, Lansbury PT.Models of amyloid seeding in Alzheimer's disease and scrapie: mechanical truths and physiological consequences of time-dependent solubility of amyloid proteins. Ann Rev Biochem 1997; 66: 385-407.
32. Hyman BT, West HL, Rebeck GW, Buldyrev RN, Mantegna M, Ukleja M, Harlin S, Stanley HE. Quantitative analysis of senile plaques in Alzheimer's disease: observation of log-normal size distributions associated with apolipoprotein E genotype and trisomy 21 (Down's syndrome). Proc Natl Acad Sci USA 1995; 92: 3586-3590.
33. Jellinger KA, Bancher C. Neuropathology of Alzheimer's disease: a critical update. J Neural Transm 1998; 54: 77-95.
34. Kawai M, Cras P, Perry G. Serial reconstruction of β-protein amyloid plaques: relationship to microvessels and size distribution. Brain Res 1992; 592: 278-282.
35. Kuner P, Bohrmann B, Tjernberg LO, Naslund J, Huber G, Celenk S, Gruninger-Leitch F, Richards JG, Jakob-Roetne R, Kemp JA, Nordstedt C. Controlling polymerization of beta-amyloid and prion-derived protein with synthetic small molecular ligands. J Biol Chem 2000; 275: 1673-1678.
36. Li GY, Zhou P, Shao ZZ, Xie X, Chen X, Wang HH, Chunyu LJ, Yu TY. The natural silk spinning process: A nucleation-dependent aggregation mechanism. Eur J Biochem 2001; 268: 6600-6606.
37. Ma J, Yee A, Brewer B, Kayyali U, Potter H. Amyloid-associated proteins β1-antichymotrypsin and apolipoprotein e promote assembly of Alzheimer β-protein into filaments. Nature 1994; 372: 92-94.
38. Maggio JE, Stimson ER, Ghilardi JR, Allen CJ, Dahl CE, Whitcomb DC, Vigna SR, Vinters HV, Labenski ME, Mantyh PW. Reversible in vitro growth of Alzheimer's disease β-amyloid plaques by deposition of labeled amyloid peptide. Proc Natl Acad Sci USA 1992; 89: 5462-5466.
39. Mann DMA, Esiri MM. The pattern of acquisition of plaques and tangles in the brains of patients under 50 years of age with Down's syndrome. J Neurol Sci 1989; 89: 169-179.
40. McKeith IG, Galasko D, Kosaka K, Perry EK, Dickson DW, Hansen LA, Salmon DP, Lowe J, Mirra SS, Byrne EJ, Lennox G, Quinn NP, Edward-

son JA, Ince PG, Bergeron C, Burns A, Miller BL, Lovestone S, Collerton D, Jansen ENH, Ballard C, de Vos RAI, Wilcock GK, Jellinger KA, Perry RH. Consensus guidelines for the clinical and pathological diagnosis of dementia with Lewy bodies (DLB): Report of the consortium on DLB international workshop. Neurology 1996; 47: 1113-1124.

41. Mirra SS, Heyman A, McKeel D, Sumi SM, Crain BJ, Brownlee LM, Vogel FS, Hughes JP, van Belle G, Berg L. The consortium to establish a registry of the neuropathological assessment of Alzheimer's disease (CERAD). II. Standardization of the neuropathological assessment of Alzheimer's disease. Neurology 1991; 41: 479-486.
42. Miyakawa T, Katsuragi S, Yamashita K, Ohuchi K. Morphological study of amyloid fibrils and preamyloid deposits in the brain with Alzheimer's disease. Acta Neuropathol 1992; 83: 340-346.
43. Motte J, Williams RS. Age-related changes in the density and morphology of plaques and neurofibrillary tangles in Down syndrome brain. Acta Neuropathol 1989; 77: 535-546.
44. Olichney JM, Hansen LA, Galasko D, Saitoh T, Hofstetter CR, Katzman R, Thal LJ. The apolipoprotein E epsilon 4 allele is associated with neuritic plaques and cerebral amyloid angiopathy in Alzheimer's disease and Lewy body variant. Neurology 1996; 47: 190-196.
45. Pollard JH. Numerical and Statistical Techniques. Cambridge University Press, Cambridge 1979, pp 97.
46. Rana AQ, Yousuf MS, Naz S, Qa'aty N. Prevalence and relation to dementia to various facators in Parkinson's disease. Psych Clin Neuro 2012; 66: 64-68.
47. Robbins EM, Betensky RA, Domnitz SB, Purcell SM, Garcia-Alloza M, Greenberg C, Rebeck GW, Hyman BT, Greenberg SM, Frosch MD, Bacskai BJ. Kinetics of capillary amyloid angiopathy progression in a transgenic mouse model of Alzheimer's disease. J Neurosci 2006; 26: 365-371.
48. Rose PE. Improved tables for the evaluation of sphere size distributions including the effect of section thickness. J Microsc 1980; 118: 135-141.
49. Saunders A, Strittmater W, Schmechel D, St. George-Hyslop P, Pericak-Vance M, Joo S, Rose B, Gasella J, Crapper-MacLachan D, Albersts M, Hulette C, Crain B, Goldgaber D, Roses A. Association of apolipoprotein E allele e4 with late-onset familial and sporadic Alzheimer's disease. Neurology 1993; 43: 1467-1472.
50. Schneider JA, Watts RL, Gearing M, Brewer RP, Mirra SS. Corticobasal degeneration: neuropathology and clinical heterogeneity. Neurology 1997; 48: 959-969.
51. Spargo E, Luthert PJ, Anderton BH, Bruce M, Smith D, Lantos PL. Antibodies raised against different proteins of A4 protein identify a subset of plaques in Down's syndrome. Neurosci Lett 1990; 115: 345-350.
52. Stanley HE, Buldyrev SV, Cruz L, Gomez-Isla T, Havlin S, Hyman BT, Knowles R, Urbanc B, Wyart C. Statistical physics and Alzheimer's disease. Physica A 1998; 249: 460-471.
53. Tierney MC, Fisher RH, Lewis AJ, Zorzitto ML, Snow WG, Reid DW, Nieuwstraten P. The NINCDS-ADRDA work group criteria for the clinical diagnosis of probable Alzheimer's disease. Neurology 1988; 38: 359-364.
54. Urbanc B, Cruz L, Buldyrev SV, Havlin S, Irizarry MC, Stanley HE, Hyman BT. Dynamics of plaque formation in Alzheimer's disease. Biophys J 1999a; 76: 1330-1334.
55. Urbanc B, Cruz L, Buldyrev SV, Havlin S, Hyman BT, Stanley HE. Dynamic feedback in an aggregation-disaggregation model. Physic Dev E 1999b; 60: 2120-2126.
56. Weibel ER. Stereological Methods. Academic Press, London 1979, pp. 123-124.
57. Wisniewski KE, Wisniewski HM, Wen GY. Ocurrence of neuropathological changes and dementia of Alzheimer's disease in Down's syndrome. Ann Neurol 1985; 17: 278-282.